

## ATR-FTIR Spectroscopic Imaging of Protein Crystallization

K. L. Andrew Chan,<sup>1</sup> Lata Govada,<sup>2</sup> Roslyn M. Bill,<sup>3</sup> Naomi E. Chayen\*<sup>2</sup> and Sergei G. Kazarian\*<sup>1</sup>

<sup>1</sup> Department of Chemical Engineering, Imperial College London, SW7 2AZ, United Kingdom

<sup>2</sup> Department of Bio-Molecular Medicine, SORA Division, Faculty of Medicine, Imperial College London, SW7 2AZ, United Kingdom

<sup>3</sup> School of Life and Health Sciences, Aston University, Aston Triangle, Birmingham B4 7ET, United Kingdom

### Abstract

Protein crystallization is of strategic and commercial relevance in the post-genomic era, due to its pivotal role in structural proteomics projects. Although protein structures are crucial for understanding the function of proteins and to the success of rational drug design and other biotechnology applications, obtaining high quality crystals is a major bottleneck to progress. The major means of obtaining crystals is by massive-scale screening of a target protein solution with numerous crystallizing agents. However when crystals appear in these screens, one cannot easily know if they are crystals of protein, salt or any other molecule that happens to be present in the trials. We present here a method based on ATR-FTIR imaging that reliably identifies protein crystals through a combination of chemical specificity and the visualising capability of this approach, thus solving a major hurdle in protein crystallization. ATR-FTIR imaging was successfully applied to study the crystallization of thaumatin and lysozyme in a high-throughput manner, simultaneously from six different solutions. This approach is fast as it studies protein crystallization *in situ* and provides an opportunity to examine many different samples under a range of conditions.

## INTRODUCTION

Determination of protein structures is key to understanding the function of proteins which are of industrial and medical interest. The most powerful method for determining the structure of proteins is x-ray crystallography which is totally reliant on the availability of high quality crystals.<sup>1</sup> Structural proteomics, which aims to determine the structures of thousands of proteins, has therefore generated great pressure to produce suitable crystals.

The past six years have seen major achievements in the field of protein crystallization. Progress in the miniaturisation and automation of crystallization experiments is making it possible to deal with the overwhelming numbers of proteins that are handled. It is now feasible to screen thousands of potential crystallization conditions by dispensing trials consisting of nanolitre volumes in a high throughput mode. This has cut the time of setting up experiments from weeks to minutes, a scenario that was unimaginable a few years ago.<sup>2</sup> However, in spite of the ability to generate numerous trials, so far only a small percentage of the proteins produced have led to structure determination. High throughput has not yet resulted in high output.

Table 1 shows a summary of results from most of the structural genomics/proteomics projects worldwide on 5<sup>th</sup> January 2009, demonstrating the attrition rate on going from cloned gene to structure. The results demonstrate that even when proteins can be expressed and made highly pure and soluble, this still does not guarantee useful crystals which will lead to structures.

**Table 1. Summary of all Major Structural Genomics Projects on 2 March 2009**

<b>Cloned</b>	139333
<b>Expressed</b>	92998
<b>Soluble</b>	36317
<b>Purified</b>	33365
<b>Diffracting crystals</b>	5894
<b>Structure defined</b>	4258

From <http://targetdb.pdb.org>

**Summary of all Major Structural Genomics Projects on 2 April 2009**

<b>Cloned</b>	142611
<b>Expressed</b>	95825
<b>Soluble</b>	36717
<b>Purified</b>	34229
<b>Diffracting crystals</b>	6175
<b>Structure defined</b>	4445

From <http://targetdb.pdb.org>

The first step in obtaining crystals is to expose the proteins to be crystallized to numerous different crystallization agents in order to identify potential crystallization conditions. Once a “hit” deemed to be conducive to crystallization is identified, conditions are optimised in an attempt to obtain high quality crystals for subsequent structural analysis. Surprisingly, crystals or crystalline precipitate are routinely considered leads that are worth pursuing. A very common problem, however, is that when one can see crystals there is no simple way of knowing if they are crystals of

protein or of another molecule arising from the crystallization agents, such as salt. In order to know definitively, one must x-ray them, but if they are too small even in one dimension, no crystal will x-ray properly. This means that one needs to obtain larger versions of these crystals which can waste a considerable amount of time, effort and consumables on possibly optimising the wrong conditions, and, the often inevitable frustration of harvesting crystals and x-raying them just to find out that they are not protein crystals. It is therefore vital to have reliable methods to distinguish between protein and other types of crystals.

Currently, several methods are available to indicate whether crystals are proteinaceous without having to x-ray them, but all have drawbacks. One method involves inserting a Coomassie Brilliant Blue dye into the crystallization drop which will colour protein crystals blue, but this method is intrusive and may harm the crystals. Another means is called the 'crush test' whereby crystals are touched with a needle. If they disintegrate easily they are likely to be protein which means that a precious protein crystal is lost. However, it can also mean that the disintegrated crystals are of the buffer or an additive that is in the trial.

With respect to spectroscopic methods, again, several options have been explored. A recent method to distinguish between salt and protein crystals is UV fluorescence imaging,<sup>3, 4</sup> which results from fluorescing amino acids in a protein. Most of the intrinsic fluorescence emissions of a folded protein are due to excitation of tryptophan residues. However, disulfide bonds also have appreciable absorption in this wavelength range. Thus, any observed UV fluorescence could also be accounted for by some additive or other molecule that is not necessarily protein contributing to the spectral response. [This problem may not be widespread, since disulfide bonds are not always present in additives, and in the cases when they are present and absorb UV radiation then they may not necessarily fluoresce at the same wavelength as proteins.](#)

In contrast, chemical imaging, based on infrared spectroscopy, has much greater chemical specificity due to characteristic absorption bands in the infrared region,<sup>5</sup> and provides an opportunity not only to identify protein crystals but also to determine secondary structures of proteins. In this paper we present a method, based on Attenuated Total Reflection (ATR)–Fourier Transform Infrared (FTIR) spectroscopic imaging, that has not been used for protein crystallization screening to date and can

reliably distinguish protein crystals from any other type of crystals in arrays of small volume (< 1microlitre) crystallization drops. The novel use of ATR-IR presented here is for *screening* to analyse whether any crystals or precipitates that are formed contain protein. This information informs a decision on whether the conditions are worth pursuing and optimising. Subsequent steps are then done outside the ATR-IR apparatus in crystallization vessels appropriate for specific crystal optimisation.

FTIR spectroscopy is known as a powerful analytical method to analyse a wide range of materials. The infrared spectra of different materials are very specific and can be used as fingerprints for their identification. The advancement in multi-pixel infrared detectors (the focal plane array or FPA detector) has brought fast imaging capability to this analytical tool with the measurement of thousands of spectra simultaneously in a few minutes or even seconds.<sup>6,7</sup> This allows the measurement of chemically-specific images without the need of added dye or stain. The appropriate comparison with ATR-FTIR imaging as a screening technique would be a confocal Raman microscopy. Chemically-specific confocal Raman spectroscopy can also be applied *in situ* to differentiate protein crystals,<sup>8</sup> but it requires much longer measurement times (because it is not an imaging approach) and also time for preparation prior to the measurement. Each crystal has to first be located under the confocal microscope and conditions (confocal depth, laser power, exposure time, etc.) need to be optimised before a decent spectrum is obtained. Confocal Raman microscopy is not amenable to imaging of many wells simultaneously, but rather consequently where each sample is measured separately. Although wet samples are often regarded as challenging samples for infrared spectroscopy due to the strong absorption of water in the mid-IR region, this has been overcome when using ATR as the sampling method. In ATR measurements, the effective pathlength is determined by the refractive indices of the internal reflection element, the wavelength and the angle of incidence of infrared light.<sup>9</sup> In general, the ATR approach would result in an effective pathlength of a few micrometers which is suitable for the measurement of wet samples or aqueous solutions. Previous studies have successfully utilised the advantage of ATR-FTIR imaging to study dissolution of tablets and pharmaceutical formulations in water.<sup>10,11</sup> It is also important to note that with a macro ATR-FTIR imaging approach described

here it is not necessary to employ a microscope unlike with confocal Raman microscopy.

In this work, we apply this methodology to study protein crystallization from a supersaturated protein solution. There are mainly two advantages using ATR-FTIR imaging for this. The first advantage is that protein and other types of crystals are readily distinguishable with FTIR spectroscopy without ambiguity. No dye or any additives are needed for the identification purpose. Infrared spectra of protein crystals can be extracted from the imaging measurement for further analysis. Secondly, samples are being measured *in situ* therefore there is no need to retrieve samples from the cultivating environment. Measurements can also be made at any time during the cultivation for the possible detection of early onsets of protein crystals. We also demonstrate the possibility of measuring multiple samples deposited in an array to render this approach readily applicable for high-throughput optimisation.

## EXPERIMENTAL SECTION

**Materials.** Three proteins were tested: lysozyme, thaumatin and the membrane protein, CD81. A solution of lysozyme was prepared at 60mg/mL by dissolving 180 mg lysozyme powder from Sigma (L6876) in 3 mL of sodium acetate buffer at pH 4.6. 6 % w/v sodium chloride (from Sigma) was prepared by dissolving the powder in deionised water. 0.8-1  $\mu$ L crystallization drops were made by mixing equal volumes of the protein and salt solutions. Thaumatin solution was prepared at 30 mg/mL by dissolving 6 mg of thaumatin powder (SigmaT7638) in 200  $\mu$ L 0.1M Bis-Tris pH 6.8 (BDH). 0.8  $\mu$ L crystallization drops were made by mixing equal volumes of the protein solution with 1.1M sodium potassium tartrate (BDH). The membrane protein CD81 was prepared as described.<sup>12</sup> Since CD81 protein has a very low solubility in water, the detergent  $\beta$ -octylglucoside was added to the protein solution prior to subjecting it to crystallization trials following a 'lead' found by routine mass screening. 0.8  $\mu$ L drops were made by mixing equal volumes of the protein and the 'lead' crystallizing solution of 0.2M calcium chloride, 45 % MPD and 0.1 M Bis-Tris pH 5.5. Paraffin oil was purchased from BDH Laboratory Supplies. All experiments were set up at 20 °C. X-ray diffraction measurements were made on a PX scanner from Oxford Diffraction.

**Instrumentation.** For the measurement of a single sample per image, 0.5  $\mu\text{l}$  protein solution was manually deposited directly onto the measuring surface of the ATR element (coupled with a ZnSe crystal accessory (Oil Analyzer, Specac Ltd) having an imaged area of approximately  $2.5 \times 3.6 \text{ mm}^2$ , and a diamond accessory (Golden Gate, Specac Ltd) adapted for imaging experiments with an imaged area of approximately  $600 \times 800 \mu\text{m}^2$ ) which is supersaturated by adding an equal amount of salt solution. The protein and salt solution mixture was sealed by surrounding the solution drop with paraffin oil (see Fig. 1, Scheme 1). For the measurement of multiple samples (i.e. in a high-throughput manner), a wax grid was first printed onto the measurement surface of the internal reflection element by using the microdroplet system (AutoDrop<sup>®</sup>, MicroDrop, Germany), creating square mini wells with dimensions of approximately  $1 \text{ mm} \times 1 \text{ mm}$  each separated by  $0.2 \text{ mm}$ . Paraffin oil was then added to cover all mini wells followed by the injection of individual protein solution into the mini well underneath the surface of the oil (Fig. 1, Scheme 2). The sample was then incubated at room temperature ( $22 \text{ }^\circ\text{C}$ ). The ATR-FTIR images were acquired using a continuous scan FTIR spectrometer in combination with a  $64 \times 64$  pixel focal plane array (FPA) detector. The number of inactive detector elements was less than 2 %. The background spectra were collected with a clean ATR crystal (i.e. without sample present). The ATR-FTIR imaging spectrometer is patented by Varian.<sup>13</sup> The spectral resolution measured was  $8 \text{ cm}^{-1}$ . 64 co-added interferograms were used to achieve a good signal to noise ratio which requires approximately 100 seconds for the simultaneous acquisition of 4096 infrared spectra.

## RESULTS AND DISCUSSION

**Strategy of sample deposition.** The arrangements of the ATR measurement are illustrated in the schematic diagram (Schemes 1 and 2 in Fig. 1). Any substances that came close to the ATR measuring surfaces (within a few micrometers) within the field of view were captured in the image. There are two possible schemes for the sample deposition. Scheme 1 shows the deposition of the protein solution before submerging in paraffin oil which provides better control of the location of the protein solution on the measuring surface. Scheme 2 shows depositing the sample drop on the measuring surface which is already covered with paraffin oil. This reduces the amount

of water evaporation giving more control of the concentration in the solution, during the sample deposition procedure. Since a typical protein solution has a higher density than the oil, the sample drop sinks to the measuring surface automatically. ATR-FTIR imaging measurements of sample prepared following the procedure described in Scheme 2 showed no detectable amount of oil present between the measuring surface and the protein solution. It should be noted that the penetration depth of the evanescent wave of the ATR-FTIR imaging approach depends on the refractive index of the medium. This may complicate its use in studies of multi-component systems. However, the difference in refractive indices here is not significant since the refractive index,  $n$ , for water is 1.33 and for proteins is 1.45 -1.5. From our previous ATR-FTIR imaging studies in aqueous solutions (e.g. tablet dissolution, diffusion, wet tissue studies<sup>10, 11</sup> and live cancer cells,<sup>14</sup>) this difference does not significantly affect the results as ATR-FTIR imaging probes the surface layer of the sample which has a thickness of only several micrometers.

**Model study – a feasibility test.** The feasibility of this measurement approach was first examined using the crystallization of lysozyme from a supersaturated solution which is the bench-mark for new protein crystallization techniques. 60 mg/mL lysozyme protein solution in sodium acetate buffer pH 4.6 was supersaturated by injecting an equal amount of precipitant solution containing 6 % NaCl to the sample protein solution. Under these conditions, lysozyme crystallizes within 1 day of incubation. Scheme 1 was applied in this experiment. After 1 day of incubation, crystals were formed from the solution and the visible image is shown in Fig. 2b. The corresponding ATR-FTIR image is shown in Fig. 2a. The ATR-FTIR image is generated by plotting the distribution of the absorbance of the protein-specific amide II band at  $1550\text{ cm}^{-1}$  across the whole imaged area. The colour on the image corresponds to the absorbance of the specific band chosen. Red regions shown in the image represent a high protein concentration in those areas, thus giving direct evidence that the precipitated crystals are protein. The location of the crystal shown in the visible image (Fig. 2b) coincides well with the FTIR image indicating that most of the protein crystals were formed very close to the measuring surface and were measured by this imaging method. From Fig. 2c, which is an overlay of Fig. 2a and 2b, the percentage of crystals captured by this imaging method was determined to be approximately 90 % for this particular protein. There are slight mismatches for three



of the protein crystals which are circled in Fig. 2c. Since the visible image was taken after the ATR-FTIR measurement, they could be caused by migration of these three crystals during movement of the ATR accessory between spectrometer and microscope. ~~Using the same procedure, protein crystals of thaumtin were also detected (data not shown, as results are similar to those in Fig. 2).~~ These simple experiments demonstrate that protein crystals can be detected once they are formed at the measuring surface and their authenticity can be verified by their infrared spectra. These crystals were not used for x-ray, but rather informed our choices in crystal optimization to achieve x-rayable crystals for subsequent analysis.

**High-throughput application.** The ATR-FTIR image in Fig. 2 showed that there are large redundant areas in the image field of view that may be utilised to measure more than one sample at a time. We have previously demonstrated that ATR-FTIR imaging is suitable for high-throughput experiments,<sup>15</sup> thus allowing screening to be done in parallel with precipitate identification. Sample preparation is simple as samples only need to make contact with the surface of the ATR element. To prevent cross contamination, samples were separated by the mean of a grid which was constructed by printing a wax wall array (solid at room temperature) from heated wax directly onto the ATR element which formed 6 mini wells within the imaging area. Samples were deposited manually into each mini well but it could also be deposited with a robotic arm.<sup>15</sup> Scheme 2 was applied in this study. Fig. 3 shows the ATR-FTIR result for 6 lysozyme solutions (even more samples may be screened in the same batch as discussed below). Each of the samples contained different protein and salt concentrations. In Fig. 3a, the locations of the sample are marked by the blue area in the oil distribution image. Note that the image shows no oil penetrated into the protein solution drop or the interface between the protein solution and the ATR measuring surface. All pixels on the image were measured simultaneously and all samples were essentially under identical conditions, allowing direct comparison of the crystallization process between protein solutions of different formulation to be made. There was no protein crystal present at the beginning of the experiment as demonstrated in Fig. 3b which was generated by plotting the absorbance of the amide II band. The image taken 18 h after the initiation of supersaturation (Fig. 3c) showed that only the sample with 30 mg/ml protein and 3.5 % NaCl formed some protein

crystals. The high-throughput study showed that this imaging method can be used as a tool to screen multiple samples and conditions for growing large monolith protein crystals.

**Diamond ATR accessory for higher spatial resolution imaging.** The spatial resolution of the FTIR images presented in Fig. 2 and 3 was approximately 40  $\mu\text{m}$  because a relatively large inverted prism made of ZnSe was used, meaning that protein crystals were detected only when they grew to a size of 40  $\mu\text{m}$  or larger. ATR-FTIR imaging with better spatial resolution would extend the application of this imaging method to detect protein crystals that grow to limited sizes or to detect early stages of ~~crystallisation~~crystallization. Previous work has demonstrated that it is possible to obtain ATR-FTIR images with higher spatial resolution that can resolve features as small as 12  $\mu\text{m}$  using a diamond ATR accessory with 4x magnification optics.<sup>14, 16, 17</sup> The same lysozyme protein solution was used in this demonstration and Scheme 1 was applied in this experiment. Fig. 4 shows the result of the *in situ* measurement of lysozyme protein crystallization using such an accessory. The image was measured 5 h after the initiation of supersaturation by mixing the protein solution with the salt solution. By using this accessory, smaller crystals which were not detected using the inverted ZnSe prism were now detectable. By improving the spatial resolution with imaging optics, the sensitivity of this method was increased. The overlaid image showed a 100% overlap between the visible and ATR-FTIR image. Nevertheless, the use of an inverted ZnSe prism is probably more suitable for high-throughput studies because it images a greater field of view.

The number of solutions that can be studied in a single batch is limited by the imaging area. The size of the image is limited by the size of the detector and the measuring internal reflection element available. The current detector contains 64 x 64 pixels offering a field of view of approximately 2.5 mm x 3.6 mm which is a fraction of the area of the ZnSe internal reflection element that is used for imaging purposes. A recent development of this ATR-FTIR imaging technique allows the internal reflection element to be translated along or across the infrared beam which enables different parts of the crystal surface to be imaged.<sup>18</sup> It has been demonstrated that the area that can be surveyed in the current setup was over 10 times the size of the image

shown in Fig. 2. It would therefore be possible to screen over 60 protein solutions in one experiment using this imaging technology.

**Crystallization of thaumatin.** To demonstrate the feasibility of applying this method to study the crystallization of ~~more-challenging~~ other proteins, thaumatin was crystallized and measured using the same procedure developed. The protein was set to crystallize on both the ZnSe ATR accessory and the diamond ATR accessory. Crystals of ~100  $\mu\text{m}$  and ~10-40  $\mu\text{m}$  in length were formed 48 hours and 24 hours after the initiation of crystallization on the two surfaces, respectively on the ZnSe and diamond surfaces. Spectra extracted from the area where these crystals were located have confirmed that they were protein crystals. The image generated by plotting the absorbance of the amide II band across the imaged area reveals the location of these protein crystals. The ATR-FTIR images have been overlaid with the corresponding visible images and the results (shown in Fig. 5) confirm that the spectra extracted were measured from the crystal deposit. This experiment ~~ensures~~ supports that the wider applicability of our imaging method is suitable for different protein solutions.

**Membrane protein study.** To demonstrate how this approach could aid protein crystallization studies for ~~challenging-membrane~~ protein targets, human CD81, was studied which is a member of the tetraspanin family of 4 transmembrane domain proteins. These proteins are involved in multiple biological functions, including cell proliferation and cell-cell adhesion, as well as being key players in cancer, the immune system, fertilisation and several infectious diseases including Hepatitis C.<sup>19</sup> Consequently CD81 and its family members are hot drug targets. Unfortunately, the production of recombinant human membrane proteins in yields sufficient for crystal trials is an enduring bottleneck in modern structural genomics programmes with CD81 being one of only relatively few examples that can be produced in a functional form in milligramme quantities.<sup>12</sup> Consequently the number of membrane protein structures is tiny compared to the situation for soluble proteins.

Crystalline structures with dimensions of ~20 x 50 x 5  $\mu\text{m}$  were formed after 24 h incubation but it was not possible to determine the identity of these crystals by light microscopy alone (see Fig. 65a). Spectra extracted from the “crystal” regions, which are shown in Fig. 65b, did not resemble the spectrum of protein. Hence, it was clear that these were not protein crystals, as confirmed by x-ray diffraction which showed the crystals to be salt.

## CONCLUSIONS

The experiments described above have clearly demonstrated that ATR-FTIR imaging can be a valuable tool, readily applicable to protein crystallization research which reduces the cost and effort required for the identification of protein crystals. It definitively determines if a ‘lead’ obtained in a screen is worth optimising. The main advantage of this technique is that identification of protein crystals can be performed *in situ*, as the crystals form, without the need to disturb the sample. This is especially important when crystallizing challenging proteins from complex systems such as ~~thaumatin and~~ the ~~one~~ demonstrated ~~in the~~ membrane protein ~~study~~. When crystals are formed, the spectrum extracted from the image can be used as a direct indicator to distinguish protein from salt or precipitants. For screening purposes, this method is even superior to x-raying the crystals which requires the crystal to have a minimum size in 3 dimensions. In contrast ATR-FTIR imaging can detect whether a crystal is comprised of protein even if it is essentially a 2D crystal, with a thickness in the z-direction of only 1  $\mu\text{m}$ . The possibility of applying this method in a high-throughput manner is particularly exciting as it will determine which conditions are worth pursuing for further crystal optimisation to yield high quality x-rayable protein crystals for structure analysis.

## ACKNOWLEDGEMENTS

NEC acknowledges the UK Engineering and Physical Sciences Research Council (EPSRC) and together with RMB the European Commission OptiCryst Project

LSHG-CT-2006-037793 and E-MeP Project LSHG-CT-2004-504601 for financial support. SGK acknowledges that the research leading to these results has received funding from the European Research Council under the *European Community's Seventh Framework Programme (FP7/2007-2013)* / ERC grant agreement n° [227950].

## REFERENCES

- (1) Chayen, N. E.; Saridakis, E. *Nature Methods* **2008**, *5*, 147-153.
- (2) Chayen, N. E. *Current Opinion in Structural Biology* **2004**, *14*, 577-583.
- (3) Judge, R. A.; Swift, K.; Gonzalez, C. *Acta Cryst 2* **2005**, *D61*, 60-66.
- (4) Li, F.; Robinson, H. *Anal Bioanal Chem* **2005**, *383*, 1034-1041.
- (5) Chen, T.; Lee, M.-J.; Kim, Y. S.; Lee, S.; Kummar, S.; Gutierrez, M.; Hewitt, S. M.; Trepel, J. B.; Levin, I. W. *Anal. Chem.* **2008**, *80*, 6390-6396
- (6) Lewis, E. N.; Treado, P. J.; Reeder, R. C.; Story, G. M.; Dowrey, A. E.; Marcott, C.; Levin, I. W. *Anal. Chem.* **1995**, *67*, 3377.
- (7) Snively, C. M.; Katzenberger, S.; Oskarsdottir, G.; Lauterbach, J. *Opt. Lett.* **1999**, *24*, 1841-1843.
- (8) Noda, K.; Sato, H.; Watanabe, S.; Yokoyama, S.; Tashiro, H. *Appl. Spectrosc.* **2007**, *61*, 11-18
- (9) Harrick, N. J. *Internal Reflection Spectroscopy*; Wiley: New York, 1976.
- (10) Kazarian, S. G.; Chan, K. L. A. *Macromolecules* **2003**, *36*, 9866-9872.
- (11) Kazarian, S. G.; Chan, K. L. A. *Biochimica et Biophysica Acta* **2006**, *1758*, 858-867.
- (12) Jamshad, M.; Rajesh, S.; Stamataki, Z.; McKeating, J. A.; Dafforn, T.; Overduin, M.; Bill, R. M. *Prot Expr Purif* **2008**, *57*, 206-216.
- (13) Burka, E. M.; Curbelo, R. *US Patent, 6141100, Imaging ATR spectrometer* **2000**.
- (14) Kuimova, M. K.; Chan, K. L. A.; Kazarian, S. G. *Appl Spectrosc.* **2009**, *63*, 164-171.
- (15) Chan, K. L. A.; Kazarian, S. G. *J. Comb. Chem.* **2005**, *7*, 185-189.
- (16) Chan, K. L. A.; Hammond, S. V.; Kazarian, S. G. *Anal. Chem.* **2003**, *75*, 2140-2147.

- (17) Chan, K. L. A.; Tay, F. H.; Poulter, G.; Kazarian, S. G. *Appl. Spectrosc.* **2008**, *62*, 1102-1107.
- (18) Chan, K. L. A.; Kazarian, S. G. *Appl Spectrosc.* **2008**, *62*, 1095-1101.
- (19) Hemler, M. E. *Nat Rev Drug Discov* **2008**, *7*, 747-758.

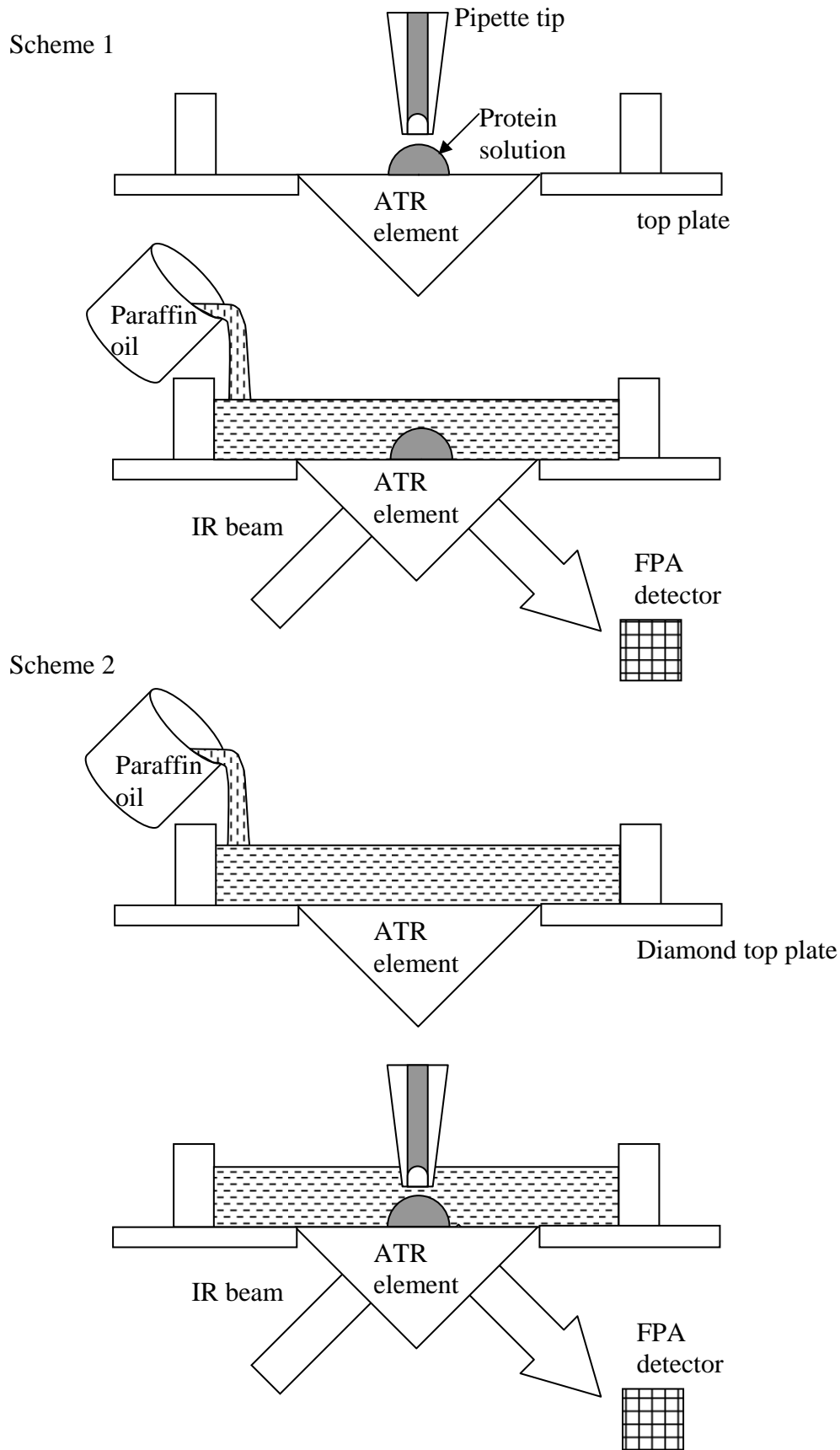


Figure 1: Schematic diagram showing different strategies for sample deposition.

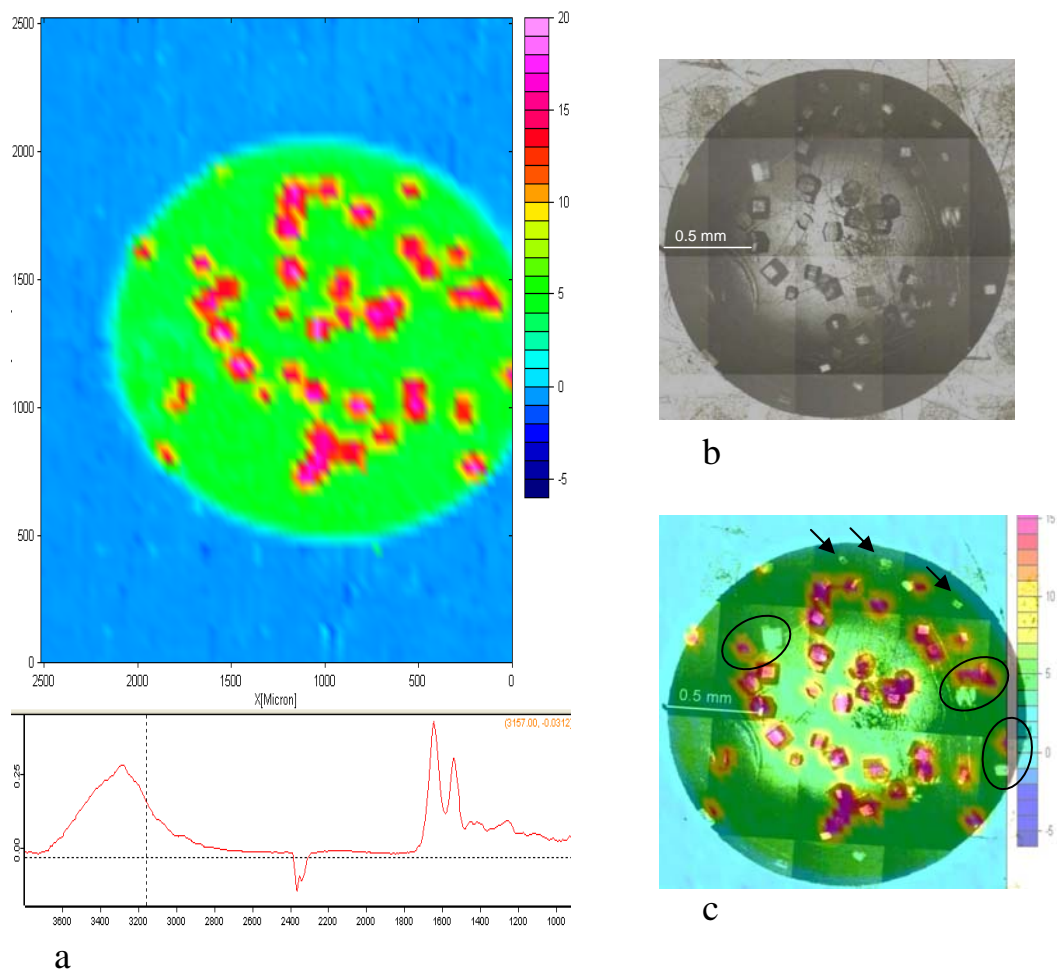


Figure 2: ATR-FTIR image (imaged area is approximately  $2.5 \times 3.6 \text{ mm}^2$ ) (a) of the protein crystal formed on the measuring surface 20 h after the introduction of the crystallizing agent. Red represents high protein concentration. The visible image (b) shows the protein crystals formed coincide well with the location of the red spots on the ATR-FTIR image. (c) Result of overlaying images (a) and (b). 5 out of 50 crystals (highlighted with arrows) were not captured in the ATR-FTIR image and 3 crystals (circled) were mislocated .



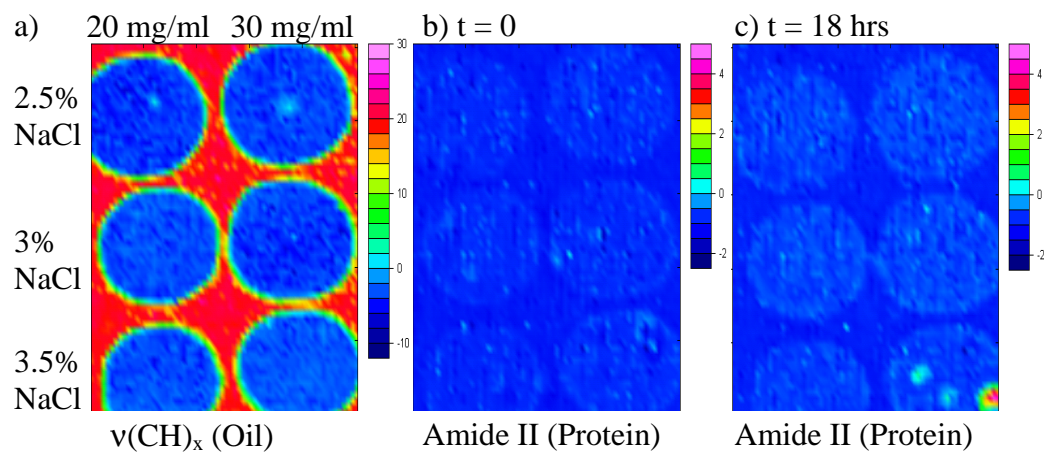


Figure 3: ATR-FTIR images of 6 different super-saturated lysozyme protein solutions at different concentrations. Image (a) represents the distribution of the surrounding paraffin oil, images (b) and (c) represent the distribution of protein (based on the amide II absorbance) at different times after the initial deposition.

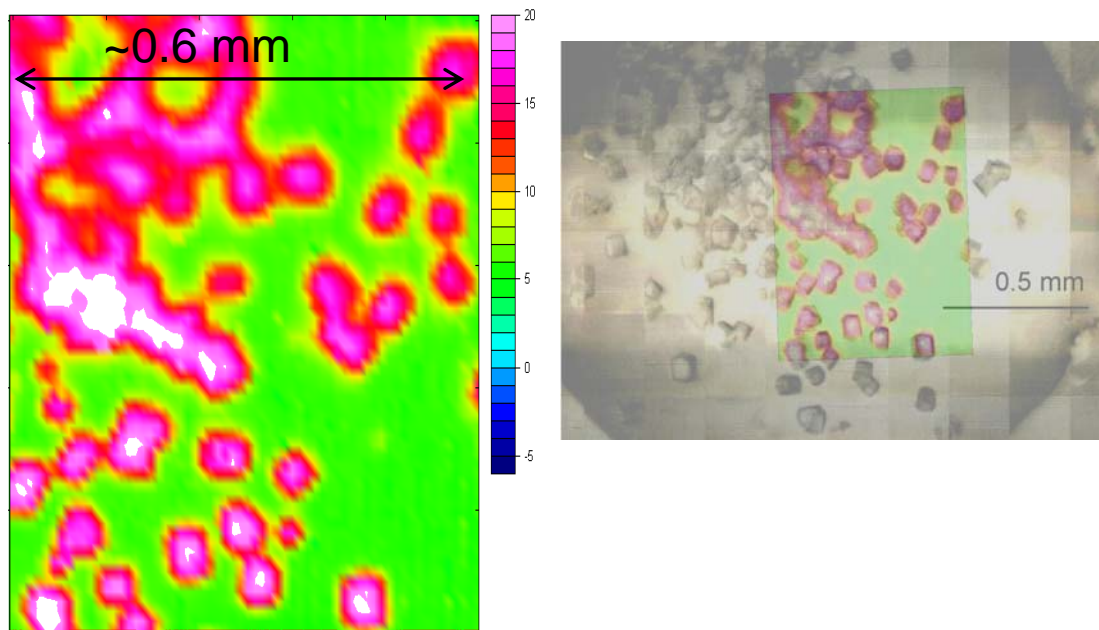


Figure 4: ATR-FTIR image (left) of the protein crystals formed on the measuring surface 5 h after the introduction of the crystallizing agent. Red represents high protein concentration. The visible image with the ATR-FTIR image overlaid (right) shows the area of measurement. The protein crystals formed coincide well with the location of the red spot on the ATR-FTIR image.

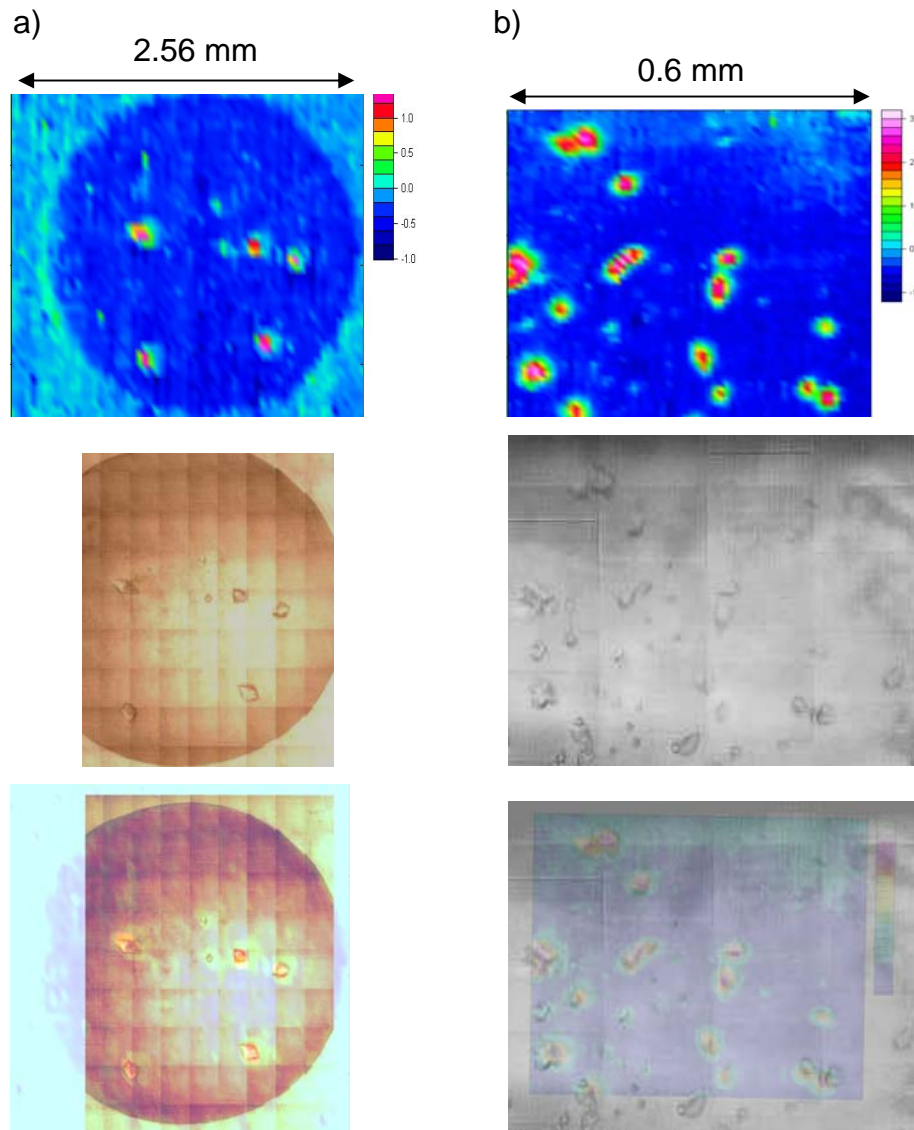


Figure 5: ATR-FTIR images (top row) of the protein (thaumatin) crystals formed on the a) measuring surface of the ZnSe ATR accessory and b) measuring surface of the diamond ATR accessory 48 and 24 hours, respectively, after the introduction of the crystallising agent. Red represents high protein concentration. The visible images (middle row) and the overlay of the ATR-FTIR and visible image-overlays (bottom row) shows the area of measurement and that the protein crystals formed coincide well with the locations of the red spots on the ATR-FTIR image.

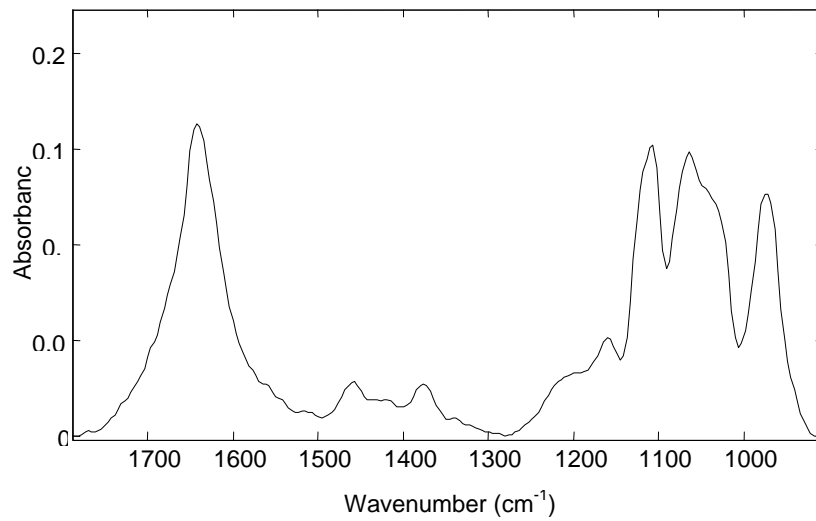


Figure 65: a) Visible image of crystal-like precipitate from the supersaturated CD81 protein solution. The length of the scale bar is 100  $\mu\text{m}$ . b) ATR-FTIR spectrum extracted from the crystal-like area of the imaging measurement.